Characteristics of Non-premixed Edge Flames in a Counterflow Slot Burner

Min Suk Cha*† and Paul D. Ronney**

ABSTRACT

The propagation rates of advancing and retreating non-premixed edge flames in a slot-jet counterflow were measured as a function of strain rate for varying jet spacing, mixture strength, stoichiometric mixture fractions (Z_{st}) and Lewis numbers (Le). Methane and propane fuels were tested and nitrogen and carbon dioxide were used as inerts. As results, we could identify igniting fronts, retreating fronts, two total extinction limits, and short-length edge flames. A burner separation affected to a low extinction limit only. Regimes for advancing and retreating edges together with total extinction were mapped in terms of normalized flame thickness and heat loss factor for $CH_4/O_2/N_2$ mixtures. Edge flames for Z_{st} > 0.5 behaved like a stronger mixture while for Z_{st} < 0.5 showed deteriorated feature, because of relative locations of a non-premixed flame and intermediate species such as CO and H_2. Furthermore, due to the relative importance of heat loss, propagating speeds of edge flames were significantly enhanced in $CH_4/O_2/CO_2$ mixtures (Le < 1) demonstrating increasing stability limits. However $C_3H_8/O_2/N_2$ mixtures (Le > 1) showed opposite result.

Key Words : edge flame, advancing, retreating, extinction limit, short-length flame.

NOMENCLATURE

d: gap spacing between burners, cm.	S_L: 1-D laminar flame speed, cm/s.
U_{edge}: propagation speed of edge, cm/s.	ρ_u: gas density of unburned mixture
σ: global strain rate, 1/s.	ρ_b: gas density of burned mixture.
Z_{st}: stoichiometric mixture fraction	ε: normalized flame thickness.
Le: Lewis number	κ: normalized heat loss factor

1. Introduction

Flames subject to temporally and spatially uniform hydrodynamic strain are frequently used to model the local interactions of flame fronts with turbulent flow fields (Williams, 1985; Peters, 1986). The "laminar flamelet" concept presumes that each surface element of the flame front behaves as though it were a steady isolated front subject to uniform strain. The applicability of laminar flamelet models in strongly turbulent flows has been questioned recently (Shay and Ronney, 1998; Liu and Ronney, 1999) because in turbulent flows the strain rate (σ) changes at rates comparable to σ itself and the scale over which the flame front curvature and σ change is comparable to the curvature scale itself. Therefore, quasi-static, local models of turbulent strain and curvature effects on laminar flamelets may not be accurate under conditions where the strain and curvature effects are most significant.

As a step towards more realistic quantification of strain effects in turbulent premixed flames, spatially uniform premixed flames subject to temporary varying strain or curvature have been studied theoretically (Huang *et al.*, 1998), computationally (Egolfopoulos,

* Korea Institute of Machinery & Materials
** University of Southern California
† corresponding author, mscha@kimm.re.kr

1994) and experimentally (Saitoh and Otsuka, 1976). The opposite case of steady flames subject to spatially-varying strain have been investigated theoretically (Daou and Lin, 1998, 1999; Vedarajan and Buckmaster, 1998; Vedarajan *et al.*, 1998) and experimentally (Shay and Ronney, 1998; Liu and Ronney, 1999). The experiments have shown that steady edge-flames can be maintained in spatially varying straining flows for both non-premixed and premixed flames. However, these studies focused on a comparison of the extinction conditions for uniformly strained flames to the strain rate corresponding to edge-flames having zero propagation speed. In order to extend the models of practical turbulent flames by incorporating the edge-flames libraries, an understanding of the dynamical properties of edge-flames is necessary. However, even in recent investigations, no retreating edge flames could be observed by experiments (Amantini *et al.* 2004).

Thus, the goal of the present investigation is to study the effects of strain rates, a burner separation distance, inert dilution rates, flame locations, and Lewis number on the propagation rates of non-premixed edge-flames and thereby to completely map dynamic and extinction properties and a stability map of edge flames with a heat loss factor, including two extinction limits, ignition fronts (advancing edges having positive speeds) and extinction fronts (retreating edges having negative speeds) on a single plot. The experimental results were then compared with those of the theoretical predictions for both ignition fronts and extinction fronts of non-premixed edge-flames (Daou *et al.*, 2002; Daou and Liñan, 1998). Finally, the effect of a gas expansion on maximum propagating speeds of edge flames will be discussed, comparing with the numerical predictions for two dimensional mixing layers (Ruetsch *et al.*, 1995)

2. Experiment

To test the propagation characteristics of edge flames in uniformly strained flow fields, we employed a counterflow slot burner. It was consisted of 13 cm 0.5 cm central rectangular nozzles, through which fuel/inert and oxygen/inert stream were ejected. At the both sides of the nozzles, there are 13 cm 0.5 cm additional slots to provide sheath flow of nitrogen. Even though the main purpose of an inert sheath is preventing a secondary diffusion flame with ambient air, in addition to this, sheath flow velocities were matched with that of the central jets to keep unspoiled strain rate from a shear with ambient. However, since the length of current nozzle is finite we had two difficulties in doing experiment 1) due to a lengthwise velocity component, ideal two-dimensional flow field is not guaranteed and 2) because there exist flame edge already, we could hardly discriminate the condition of the total extinction from extinction front (retreating edge). To solve above problems, we placed ceramic burner spacers which was assembled with hot wire (see Fig. 1) at the ends of the nozzles to suppress unwanted lengthwise velocity component, and to anchor a flame edge at the surface of the hot wire by electrical heating at the same time. The internal construction of the burners consisted of steel wool and aluminum honeycomb to ensure uniformity of the exit flow of all slots. The nozzles (and thus reactants) were maintained at room temperature by water-cooling. Commercial mass flow controllers with accuracy 1% of full scale (calibrated with wet-test meters) delivered the combustible gases to the nozzles.

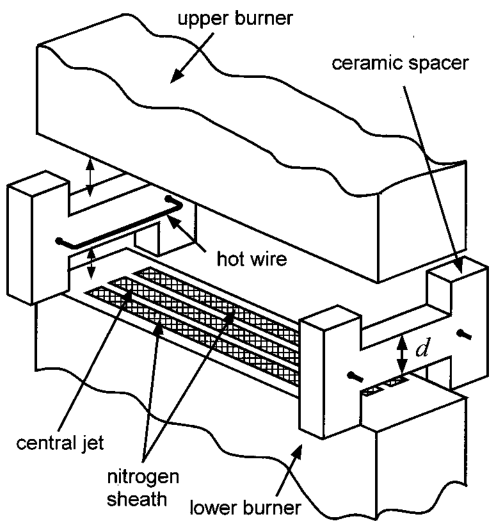

Fig. 1 Schematic of burner setup

For all experiments, the lower nozzle contained the mixture of fuel (CH_4 or C_3H_8) and inert (N_2 or CO_2) and the upper nozzle contained the mixture of oxidizer (O_2) and inert (N_2 or CO_2). For a fixed overall fuel/oxygen/inert ratio and the burner separation distance (d), we vary the nozzle exit velocity, thus strain rate. It is to be noted that the nozzle exit velocities for lower and upper nozzles were kept the same for entire experiments.

Ignition fronts (advancing edges having positive

Table 1. Experimental conditions and corresponding properties

Mixture composition (Volume ratio) (Lewis number)	Inert ratio (Q_{N2}, Q_{CO2})	S_L (cm/s)	d (cm)	Z_{st}	$(\rho_u/\rho_b)^{1/2}$	α (cm^2/s)	β
$CH_4/O_2/N_2$ (1/ 2/ Q_{N2}) (Le = 1)	6.0	57.9	0.75	0.5	2.842	0.201	9.58
	9.0	25.5	0.75	0.5	2.636	0.201	10.8
	9.5	22.2	0.5, 0.75, 1 0.75	0.5 0.2, 0.8	2.604	0.200	11.0
	10.0	19.2	0.75	0.5	2.573	0.200	11.2
	11.0	14.1	0.75	0.5	2.513	0.200	11.6
	11.75	11.0	0.75	0.5	2.470	0.200	11.9
	12.0	10.1	0.75	0.5	2.456	0.200	12.0
	12.25	9.28	0.75	0.5	2.443	0.200	12.2
	12.5	8.50	0.75	0.5	2.430	0.200	12.3
$CH_4/O_2/CO_2$ (1/ 2/ Q_{CO2}) (Le < 1)	4.09	25.2	0.50	0.5	2.766	0.133	14.0
	4.35	21.9	0.50	0.5	2.738	0.131	14.2
	4.85	16.7	0.50	0.5	2.686	0.129	14.6
	5.28	13.0	0.50	0.5	2.643	0.127	14.9
	6.50	6.07	0.50	0.5	2.528	0.123	16.0
	7.10	4.17	0.50	0.5	2.476	0.121	16.5
$C_3H_8/O_2/N_2$ (1/ 5/ Q_{N2}) (Le > 1)	16.6	56.0	0.68	0.5	2.886	0.182	9.08
	20.0	39.9	0.68	0.5	2.782	0.185	9.61
	23.0	28.7	0.68	0.5	2.696	0.186	10.0
	26.2	20.5	0.68	0.5	2.611	0.187	10.5
	27.6	17.7	0.68	0.5	2.576	0.188	10.8
	28.9	15.0	0.68	0.5	2.542	0.188	11.0

speeds) were obtained by extinguishing a steady flame from one end of the nozzle to other by sweeping a small round jet of N_2, then letting a flame edge propagate by sudden removing of N_2 jet. To obtain Extinction fronts (retreating edges having negative speeds), the hot wire of the spacer were heated electrically to anchor the flames there, and local extinction was triggered with a N_2 jet to extinguish the flame locally near one end. The propagation of the ignition and extinction fronts was recorded by a color digital video camera (framing rate 29.97 Hz, shutter speed 1/100 sec). The locations of flame edges were measured from the digitized images frame by frame and the propagation speed was determined as an interpolated value at the burner center by using least square fit of the experimental flame speed as a function of location, excluding initial short period to avoid any disturbances from extinguishing N_2 jet.

Furthermore, two extinction limits were also observed: one at low strain rates due to heat losses to the jets (heat loss limit) and another at high strain rates due to insufficient residence times (Damköhler number limit). Strain rate corresponding to the latter was obtained by establishing a uniform flame ata relatively lower stretch rate and then gradually increasing the nozzle jet exit velocity U_{jet}: the value of U_{jet} when the flame is extinguished itself provides the strain rate at the extinction limit. On the other hand, strain rate at the extinction limit caused due to heat losses was defined as the minimum strain rate, which was obtained by establishing a uniform flame at a relatively higher stretch rate and then gradually decreasing U_{jet}.

Data for the above four categories of edge-flames (ignition fronts, extinction fronts, and two extinction limits) were obtained for the experimental conditions listed in Table 1. To evaluate the effects of flame strength on the edge-flame propagation, the volume ratio of methane to oxygen was fixed at stoichiometry (volume ratio of CH_4/O_2 = 1/2) and the amount of nitrogen was varied. For the whole experiments for various flame strength with $CH_4/O_2/N_2$, burner separation distance d was kept 0.75 cm and stoichiometric mixture fraction defined as $Zst = 1/(1+\nu\, m_f/m_o)$ is fixed at 0.5 meaning that flame locates at the center of two burners. Here, ν is a stoichiometric oxygen to fuel mass ratio, m_f and m_o are initial mass fractions of fuel and oxygen for each side of stream, respectively.

To verify the effects of burner separations and relative flame locations, we choose $CH_4/O_2/N_2$ = 1/2/9.5 mixture as a representative case, then for d = 0.75 cm flame location was varied, such that Z_{st} = 0.2 (flame sits near oxidizer side upper nozzle) and Z_{st} = 0.8 (flame sits near fuel side lower nozzle). And for Z_{st} = 0.5, d = 0.5 and 1.0 cm were tested.

Finally, $CH_4/O_2/CO_2$ and $C_3H_8/O_2/N_2$ mixtures were tested to investigae the Lewis number effects. $CH_4/O_2/CO_2$ mixtures represent Le < 1, and $C_3H_8/O_2/N_2$ mixtures for Le > 1. To be a reasonable comparison with $CH_4/O_2/N_2$ mixtures, laminar burning velocities set to be same for some comparable cases and the burner separation was changed so as to have a similar Peclet number (= S_Ld/α or $U_{jet}d/\alpha$) which means keeping similar heat loss characteristics. Here, S_L is calculated by 1-D premixed code with GRI 3.0 mechanisms or Wang mechanisms for methane and propane respectively, α is a thermal diffusivity calculated by chemical equilibrium code. Table 1 also shows corresponding relevant properties, such as S_L, α, $(\rho_u/\rho_b)^{1/2}$, and Zeldovich number β (= $E(T_{ad}$ $T)/(RT_{ad}^2)$). Here, E/R was calculated by linear-curve-fitting of $\ln(S_L) = f(1/T_{ad})$. In this relation, a slope represents $E/2R$.

3. Results and Discussion

The results of the present experiments cover near every aspect of edge flames in uniformly strained flow fields, including effects of d (heat loss to the burner), mixture strength (the amount of inert dilution), flame location (different Z_{st}), and Lewis number. Most of present results will be shown with normalized propagation speeds of edge flames as a function of normalized flame thickness to compare with the results of Daou *et al.* (2002). The propagation speeds of edge flames (U_{edge}) are normalized by the flame speeds (S_L) of the premixed flames with the same composition, and the square root of the density ratio of unburned (ρ_u) to burned mixtures (ρ_b) as $U_{edge}/(S_L(\rho_u/\rho_b)^{1/2})$, which is based on the theoretical study by Ruetsch *et al.* (1995), and normalized flame thickness (ε) is defined as $\varepsilon \equiv \beta\,(\sigma\alpha/(2S_L^2))^{1/2} = \beta\,(\mathrm{Ka}/2)^{1/2}$, which is based on Daou *et al.* (2002). Here, σ is a strain rate defined as $2U_{jet}/d$ and Ka is the Karlovitz number.

3.1 Effect of burner separation

To elucidate the effects of burner separation distance on the propagation characteristics of non-premixed edge flames, we chose the volume ratio of $CH_4/O_2/N_2$ = 1/2/9.5 mixture as a reference case, then three different burner spacers, i.e., d = 0.5, 0.75, and 1.0 cm were used.

Figure 2 shows the propagation characteristics of edge flames and the lower and upper extinction limits of diffusion flames. Advancing and retreating edges are clearly demonstrated showing negative values of U_{edge} for both low and high ε. Except for low ε region, propagation and extinction characteristics for all three different d are nearly identical, which means that for high enough strain rates U_{edge} and the high extinction value of ε are not affected by d. Main controlling parameter for the edge-flame propagation is strain rate.

However, for low value of ε (thus low strain rate), as strain rate decreases advancing flame edges change to retreating edges suddenly and shortly after total extinction occurs, while for high strain rate the transition between positive and negative values of U_{edge} was smooth. This kind of low total extinction after sudden change from igniting to extinction front is most different features of the present work from a numerical study by Daou *et al.* (2002).

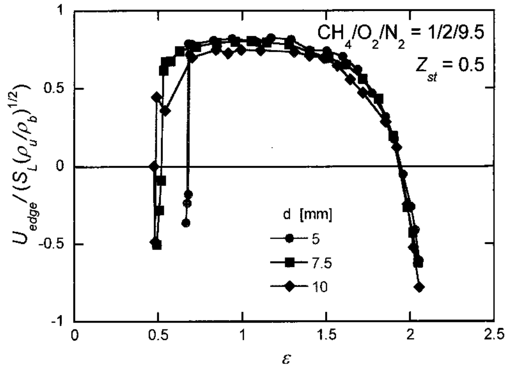

Fig. 2 Normalized U_{edge} with normalized flame thickness for $CH_4/O_2/N_2$ =1/2/9.5, Z_{st} = 0.5, and various d

These results should be affected by the heat loss to the burner, which was not counted on the work by Daou *et al.* (2002). Since a thermal boundary thickness will be proportional to $(\alpha/\sigma)^{1/2}$, $(\alpha/\sigma)/d^2 \sim \alpha/(U_{edge}d)$ = $1/\mathrm{Pe}_{burner}$ will be a appropriate nondimensional parameter to represent the degree of heat loss to the burner. However, increasing buoyancy driven convectional velocity, which will be scaled with $(gd)^{1/2}$, cold be responsible for the low extinction limit at large d. Here, g is the gravitational acceleration constant. In fact, as shown in Fig. 2, due to a convective perturbation, which should be from buoyancy, the results with d = 1.0 cm exhibit fluctuating U_{edge} for $\varepsilon < 0.7$. We can conclude that it is really hard to realize edge-flame experiments for low strain rate because of both heat loss to a burner (for small d) and buoyancy (for large d).

3.2 Effects of mixture strength

To investigate the effects of mixture strength on edge and diffusion flames, the amount of N_2 dilution was varied for $CH_4/O_2/N_2$ mixtures. The amount of N_2 dilution was increased, then no stable flames were observed for $CH_4/O_2/N_2$ = 1/2/12.5 which means that total extinction occurred for entire range of strain rate for this mixture.

Figure 3 shows the results of U_{edge} as a function of strain rate. As the amount of N_2 dilution increases, strain rate at high extinction limit is reduced and strain rate at low extinction limit is increased demonstrating reduced stability region. A maximum U_{edge} for each case was also decreased for increasing N_2 dilution, and beyond a certain mixture composition (around $CH_4/O_2/N_2$ = 1/2/11.75) only retreating edge flames can be observed. For further increasing N_2 dilution total extinction occurred for any strain rates.

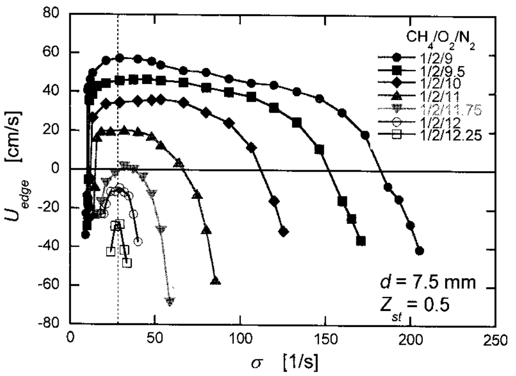

Fig. 3 U_{edge} with strain rate for d = 7.5 mm, Z_{st} = 0.5, and various N_2 dilution rate in $CH_4/O_2/N_2$ mixture

The dashed vertical line in Fig. 3 qualitatively well trace the maximum U_{edge} for each case. Though the maximum U_{edge} should be occurred at zero strain-rate excluding heat loss factor to burner (Daou *et al.* 2002), in real situations due to the heat loss to the burner, the maximum U_{edge} was observed in the intermediate strain rate, which means that the condition of the maximum U_{edge} should be strongly related with the heat loss to the burner. In this regard, we can consider the vertical dashed line as a constant Peclet number line for $CH_4/O_2/N_2$ mixture, because the thermal diffusivities of those mixtures are nearly same for tested conditions as listed in Table 1. For $CH_4/O_2/N_2$ mixtures, Pe_{burner} = 39 in the present experiments, and a comparison with other mixtures will be discussed last section.

In Fig. 4 the results of normalized U_{edge} for normalized flame thickness were shown to provide a comparison with Daou *et al.* (2002). Qualitatively, the trends of propagation and high extinction of flames are almost same, except a critical feature. In the present results, for low strain-rate (or ε) region there is sudden drop in U_{edge} (positive to negative speed) as strain-rate decreases, on the other hand sudden jump from negative to positive speed occurs in the numerical study by Daou *et al.* (2002). This difference is originated from the heat loss characteristics to the burner, which the numerical study could not include.

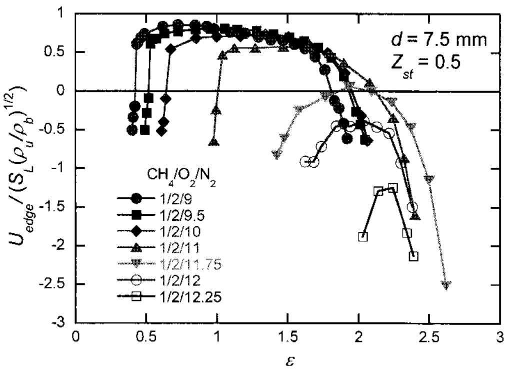

Fig. 4 Normalized U_{edge} with normalized flame thickness rate for d = 7.5 mm, Z_{st} = 0.5, and various N_2 dilution rate in $CH_4/O_2/N_2$ mixture

However, in the numerical work, edge flames in low strain-rate region are called as *tailless triple flame* even though it have positive edge speeds, which means that a trailing diffusion flame should be extinguished at the same time of propagation. In the present study, when checking the flame characteristics near the low extinction regime for decreasing N_2 dilution, a *short-length edge flame* was observed for $CH_4/O_2/N_2$ = 1/2/6 and U_{jet} = 2 cm/s (see Fig. 5). Because it has propagating leading edge and retreating trailing edge at the same time, we have to provide two different values for it, i.e., U_{edge} = 48 cm/s and -52 cm/s for leading and trailing edges, respectively.

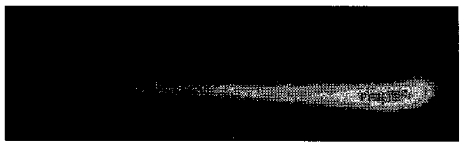

Fig. 5 False-color image of short-length edge flame taken by an ICCD camera for mixture of $CH_4/O_2/N_2$ = 1/2/6 and U_{jet} = 2 cm/s

To conclude the effects of mixture strength, we plot a flame stability map in terms of heat loss factor κ and normalized flame thickness ε following the numerical work by Daou *et al.* (2002) in Fig. 6. The heat loss factor κ was defined as $\beta(\alpha/S_L^2)\kappa_0$, here κ_0 is a linear volumetric heat loss coefficient. To determine κ_0 in the present experimental setup, we consider heat loss to two infinite parallel plates with laminar flow. Since κ_0 is a heat loss rate having unit of 1/s, κ_0 should be $hA\Delta T/(\rho C_p V\Delta T)$. Here, the heat transfer coefficient $h = 3.77\ k/d$, k is the heat conductivity, A is an area for heat transfer (= 2×geometric area of 1 plate, A_{plate}), V is the volume (= $A_{plate}\times d$). Hence, $\kappa_0 = 3.77\ (k/d)\times 2A_{plate}/(\rho C_p A_{plate} d) = 7.54\ \alpha_{avg}/d^2$, where α_{avg} has to be temperature-averaged. Using α for unburned mixture for convenience instead of α_{avg}, we can express as $\kappa = \beta(\alpha/S_L^2)(7.54\alpha/d^2) = 7.54\ \beta(\alpha/(S_L d))^2 = 7.54\beta/\mathrm{Pe}_{flame}^2$.

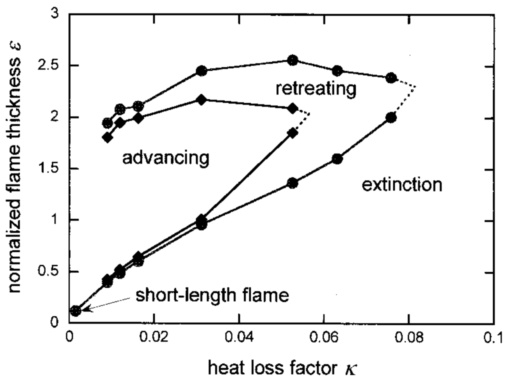

Fig. 6 Map of propagation modes and extinction limits of edge flames with heat loss factor and normalized flame thickness for $CH_4/O_2/N_2$ mixtures

As you can see in the Fig. 6, the stability domain of κ-ε plane is quite similar to the numerical work by Daou *et al.* (2002) except the high extinction limit and high transition ε for positive to negative edge in relatively low κ region and there is nearly small region for short-length edge flames. It is to be noted that the dotted lines in the figure were determined by extrapolation from strain-rate and U_{edge} domain of stability.

3.3 Stoichiometric mixture fraction

Flame location can be another parameter to affect to edge flame characteristics. Keeping the same overall mixture ratio, stoichiometric mixture fraction Z_{st} was varied for $CH_4/O_2/N_2$ = 1/2/9.5 mixture. Noting that the Lewis number of this $CH_4/O_2/N_2$ mixture can be treated as unity, we can assume the same premixed S_L and adiabatic flame temperatures for different Z_{st} (thus flame location).

The results of Z_{st} = 0.2, 0.5, and 0.8 for $CH_4/O_2/N_2$ = 1/2/9.5 mixture and d = 0.75 cm are shown in Fig. 7. As shown in the figure, as Z_{st} increases, U_{edge} increases for the same ε and the low and high extinction limits are enlarged. One might simply conceive that if the flame location is moved to one side of burner from the center of the burner separation, flame will be weaker for low strain-rate region because of enhanced heat loss effect to the burner wall. There are no differences in mechanical aspects, such as flow-field and heat loss, between Z_{st} = 0.2 and 0.8. It is likely that one might assume symmetric behavior for different Z_{st}. However, the present results say if a flame locates in the oxidizer side (Z_{st} < 0.5), it should be deteriorated, and if a flame sits on the fuel side (Z_{st} > 0.5), it must be stronger in terms of U_{edge} and extinction limits. An experimental work for extinction limits of non-premixed flames by Kitajima *et al.* (2004) reported similar results. The results were the high extinction limit is increased for increasing Z_{st}.

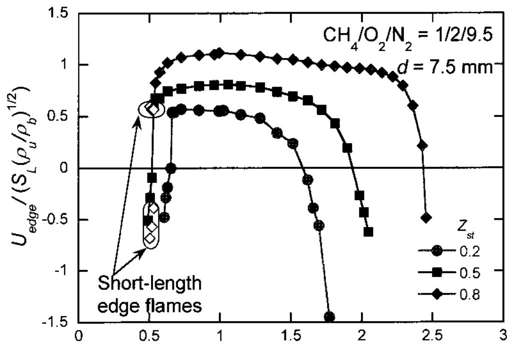

Fig. 7 Normalized U_{edge} with normalized flame thickness for $CH_4/O_2/N_2$ =1/2/9.5, *d* = 7.5 mm, and various Z_{st}

Generally, in counter flow diffusion flames, intermediate fuel species such as CO and H_2 are abundant in a fuel side (Tsuji, 1982). Considering Z_{st} = 0.8, intermediate fuel species locate upstream side of the fuel stream. Since these fuel species must pass through the flame zone by convection, there is enough heat and oxygen to oxidize these CO and H_2 fuels. While for Z_{st} = 0.2, CO and H_2 are generated downstream of the oxidizer stream, there is no heat and oxygen to be oxidized. As a result, this concentrated heat release in Z_{st} = 0.8 can make a flame be stronger, and less heat release for Z_{st} = 0.2 is responsible for weaker flame.

It is to be noted that *short-length edge flame* can be observed for Z_{st} = 0.8 near low extinction condition. In the figure, positive U_{edge} for advancing leading edges and negative U_{edge} for retreating trailing edges are plotted for the same ε as an open diamond symbol.

3.4 Effects of Lewis number

Lastly, the effects of different Lewis number on the characteristics of edge flames were investigated. $CH_4/O_2/CO_2$ mixtures were used to represent Le < 1, and $C_3H_8/O_2/N_2$ mixtures for Le > 1. Even though we tried to test with the same fuel, i.e. methane, it was found that $CH_4/O_2/He$ mixtures (Le > 1) were not eligible to be stabilized in the tested burner for the tested range of mixture strengths and strain-rates.

The results of normalized U_{edge} with ε are shown in Fig. 8. To compare with the case of Le = 1, the results of $CH_4/O_2/N_2$ = 1/2/10 having S_L = 19.2 cm/s are also plotted in the Fig. 8a. For Le > 1 case ($C_3H_8/O_2/N_2$ mixtures), U_{edge} are much smaller than the case of Le =1 at the same ε or σ comparing the cases having similar S_L = 20.5 cm/s ($C_3H_8/O_2/N_2$ = 1/5/26.2), and it shows smaller high extinction ε and large low extinction e. These results mean that the mixtures with Le > 1 behave like a weaker mixture than Le = 1 even though it have a similar S_L. It is apparent that since a heat loss to unburned streams is much higher than a mass diffusion towards a reaction zone for Le > 1, edge flames will be weaker than Le = 1.

On the other hand, now one can imagine that with a mixture of Le < 1 will show an opposite results. $CH_4/O_2/CO_2$ = 1/2/5.28 having S_L = 13.0 cm/s shows much higher normalized U_{edge} even compare to $CH_4/O_2/N_2$ = 1/2/10 with S_L = 20.5 cm/s. Since the heat loss factor κ = 0.198 for this $CH_4/O_2/CO_2$ = 1/2/5.28 case, it is twice much higher than the total extinction κ for $CH_4/O_2/N_2$ mixtures meaning that a great enhancement in flame stability. Unlike the other tested results, $CH_4/O_2/CO_2$ mixture having S_L = 13.0 and 6.07 cm/s show different U_{edge} characteristics. As ε (or σ) increases, U_{edge} increases, then reaches its maximum value followed by sudden drop. It is qualitatively similar to a numerical work by Daou and Liñan (1998). In this numerical work, the maximum value of U_{edge} occurs at zero ε (or σ) for Le 1, however it occurs at certain intermediate ε for Le < 1.

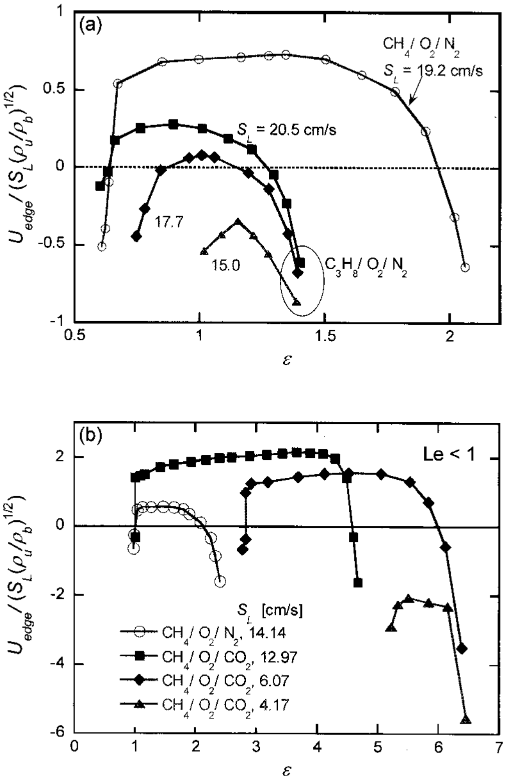

Fig. 8 Normalized U_{edge} with normalized flame thickness for $C_3H_8/O_2/N_2$ mixtures with different N_2 dilution rate, d = 6.8 mm, and Z_{st} = 0.5 representing Le > 1 (a), and $CH_4/O_2/$ CO_2 mixtures with different CO_2 dilution rate, d = 5 mm, and Z_{st} = 0.5 representing Le< 1 (b)

In previous theoretical and numerical study by Ruetsch *et al.* (1995), the proportional relation between U_{edge}/S_L and $(\rho_u/\rho_b)^{1/2}$ considering gas expansion effects on two dimensional parallel mixing layers. In this regard, U_{edge}/S_L are plotted with $(\rho_u/\rho_b)^{1/2}$ together with the results by Ruetsch *et al.* in Fig. 9. As shown in Fig. 10, in $CH_4/O_2/N_2$ and $C_3H_8/O_2/N_2$ mixtures U_{edge}/S_L demonstrate near linear proportionality to $(\rho_u/\rho_b)^{1/2}$ for advancing edges, while $CH_4/O_2/CO_2$ mixtures are not because Pe_{burner} = 39 is not a representative value for Le < 1. It is interesting to compare with the results by Ruetsch *et al.* In the present counterflow geometry, there are no flames in relatively low $(\rho_u/\rho_b)^{1/2}$ region. So, the gas expansion effects on edge flames should be considered differently for different flow configuration.

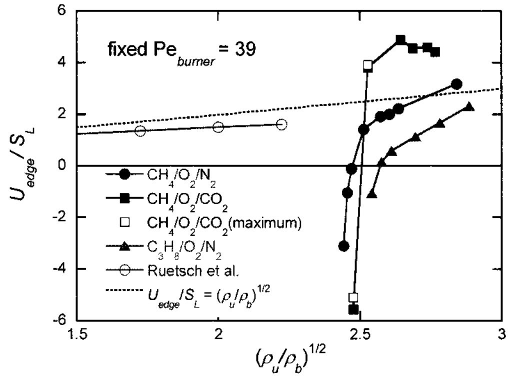

Fig. 9 U_{edge} normalized by S_L versus density ratio for Pe_{burner} = 39 representing maximum U_{edge} for a given mixture except $CH_4/O_2/CO_2$ mixture

4. Conclusions

The propagation rates of advancing and retreating non-premixed edge-flames in a slot-jet counterflow were measured as a function of strain rate for varying jet spacing, mixture strength, stoichiometric mixture fractions, and Lewis numbers. For a given mixture family, edge-flame propagation rates for different mixture strengths scaled by a thermal expansion factor and the laminar burning velocity of a stoichiometric premixture of the reactant streams correlated well with a non-dimensional flame thickness ε related to the strain rate and laminar burning velocity. For mixtures families with lower (higher) reactant Lewis numbers, the edge-flame speeds were much higher (lower). Also, edge-flame speeds were higher (lower) for higher (lower) stoichiometric mixture fractions. Two extinction limits were identified, one at low strain due to heat loss to the jets and one at high strain due to insufficient residence time for chemical reaction. The low-strain limit could be characterized solely in terms of a dimensionless heat loss parameter κ and was practically independent of all other experimental factors. The high-strain limit is strongly influenced by the reactant Lewis numbers and stoichiometric mixture fraction, but is independent of κ and thus mixture strength for a given mixture family. For some mixtures, "short-length edge-flames" were observed, but only for very narrow ranges of conditions near the low-strain extinction limits. These results are mostly consistent with theoretical predictions, except for the flame structures and propagation rates near the low-strain extinction limits. This is proposed to be due to the differences between the theoretical assumption of volumetric heat losses and the experimental situation of gradient-driven heat losses to the jet exits.

Acknowledgments

MSC was supported by the Korea Research Foundation (KRF) Grant (M01-2004-000-10055-0). The authors are grateful to M. K. Kim and S. Manasra for their valuable assistance with the experiments

References

[1] Amantini, G., Frank, J. H., Gomez, A. (2004). *Proc. Combust. Inst.* **30,** in press.
[2] Daou, R., Daou, J. and Dold, J. (2002). *Proc. Combust. Inst.* **29**, .
[3] Daou, J. and Liñan, A. (1998). *Combust. Theory and Modelling* **2**, 449.
[4] Daou, J. and Liñan, A. (1999). *Combust. Flame* **118**, 479.
[5] Egolfopoulos, F. N. (1994). *Proc. Combust. Inst.* **25**, 1365.
[6] Huang, Z., Bechtold, J. K. and Matalon, M. (1998). *Combust. Theory and Modelling* **2**, 115.
[7] Kitajima, A, Torikai, H., Takeuchi, M., and Oya, M. (2004). *Combust. Flame* **137**, 93.
[8] Liu, J.-B. and Ronney, P. D. (1999). *Combust. Sci. Tech.* **144**, 21.
[9] Peters, N. (1986). *Proc. Combust. Inst.* **21,** 1231.
[10] Ruetsch, G. R., Vervisch, L. and Linan, A. (1995). *Physics of Fluids* **7**, 1447.
[11] Shay, M. L. and Ronney, P. D. (1998). *Combust. Flame* **112**, 171.
[12] Saitoh, T. and Otsuka, Y. (1976). *Combust. Sci. Tech.* **12,** 135.
[13] Tsuji, H. (1982). *Prog. Energy Combust. Sci.* **8**, 93.
[14] Vedarajan, T. G. and Buckmaster, J. D. (1998). *Combust. Flame* **114**, 267.
[15] Vedarajan, T. G., Buckmaster, J. D. and Ronney, P. D. (1998). *Proc. Combust. Inst.* **27**, 537.
[16] Williams, F. A. (1985). *Combustion Theory*, 2nd ed., Benjamin-Cummins.